Open Access

This article is licensed under CC-BY-NC-ND 4.0

Article

Evaluating Imide-Based Mass Spectrometry-Cleavable Cross-Linkers for Structural Proteomics Studies

Alessio Di Ianni, Christian H. Ihling, Tomáš Vranka, Václav Matoušek, Andrea Sinz, and Claudio Iacobucci*

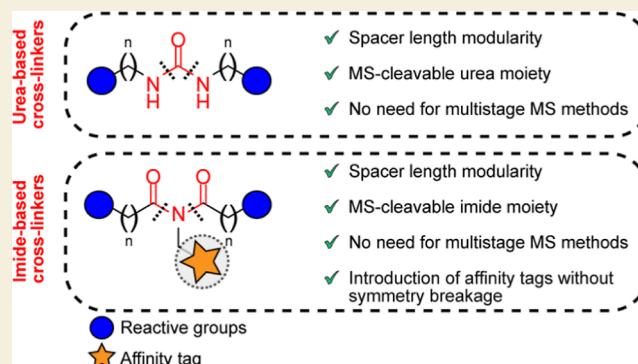Cite This: JACS Au 2024, 4, 2936−2943

Read Online

ACCESS | Metrics & More | Article Recommendations | Supporting Information

ABSTRACT: Disuccinimidyl dibutyric urea (DSBU) is a mass spectrometry (MS)-cleavable cross-linker that has multiple applications in structural biology, ranging from isolated protein complexes to comprehensive system-wide interactomics. DSBU facilitates a rapid and reliable identification of cross-links through the dissociation of its urea group in the gas phase. In this study, we further advance the structural capabilities of DSBU by remodeling the urea group into an imide, thus introducing a novel class of cross-linkers. This modification preserves the MS cleavability of the amide bond, granted by the two acyl groups of the imide function. The central nitrogen atom enables the introduction of affinity purification tags. Here, we introduce disuccinimidyl disuccinic imide (DSSI) as a prototype of this class of cross-linkers. It features a phosphonate handle for immobilized metal ion affinity chromatography enrichment. We detail DSSI synthesis and describe its behavior in solution and in the gas phase while cross-linking isolated proteins and human cell lysates. DSSI and DSBU cross-links are compared at the same enrichment depth to bridge these two cross-linker classes. We validate DSSI cross-links by mapping them in high-resolution structures of large protein assemblies. The cross-links observed yield insights into the morphology of intrinsically disordered proteins and their complexes. The DSSI linker might spearhead a novel class of MS-cleavable and enrichable cross-linkers.

KEYWORDS: cross-linking mass spectrometry, XL-MS, protein−protein interactions, structural proteomics, DSBU, intrinsically disordered protein, IDP

Urea-based cross-linkers
- ✓ Spacer length modularity
- ✓ MS-cleavable urea moiety
- ✓ No need for multistage MS methods

Imide-based cross-linkers
- ✓ Spacer length modularity
- ✓ MS-cleavable imide moiety
- ✓ No need for multistage MS methods
- ✓ Introduction of affinity tags without symmetry breaking

● Reactive groups
★ Affinity tag

INTRODUCTION

Over the past 2 decades, cross-linking mass spectrometry (XL-MS) has emerged as a powerful technique for exploring the 3D structures of proteins and protein complexes in their native environment.[1,2] Chemical cross-linkers covalently bridge two amino acids in spatial proximity and serve as molecular rulers to unveil the morphology and plasticity of proteins. The major bottleneck of XL-MS remains the analysis of the complex enzymatic proteolyzates obtained from the cross-linked sample. Cross-links are formed substoichiometrically and are dispersed in a several orders of magnitude higher concentrated background of tryptic peptides. The direct application of reverse-phase (RP) liquid chromatography coupled to tandem mass spectrometry (LC-MS/MS) does not provide a comprehensive identification of cross-links, especially in system-wide XL-MS experiments.[3]

Reducing the Sample Complexity

Adding further chromatographic dimensions enhances the depth of the analysis. Size exclusion (SEC),[4] strong cation exchange (SCX),[5] hydrophilic strong anion exchange,[6] and high-pH RP[7] chromatography leverage the increased average size and charge state of cross-links over linear peptides to prefractionate proteolyzed cross-linked samples.[8] Also, several cross-linkers incorporate molecular tags like biotin, azide,[9] alkyne,[9,10] or phosphonate,[11] enabling affinity purification of cross-links. The combination of affinity purification followed by SEC or SCX allows reducing the background of linear peptides in the sample.[12−14] Among the affinity handles, the phosphonate has recently emerged as one of the more promising options in system-wide XL-MS.[12] Phosphonate-containing cross-links can be enriched by immobilized metal ion affinity chromatography (IMAC) or on titanium dioxide (TiO₂) beads. This approach is derived from conventional phosphoproteomics and, unlike phosphopeptides, phospho-nates do not suffer from chemical or enzymatic instability.
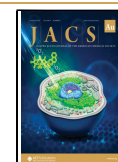
Simplifying Data Acquisition and Analysis

The complexity of cross-linked samples also affects downstream MS data analysis. Here, MS-cleavable cross-linkers like disuccinimidyl dibutyric urea (DSBU),[4,15] disuccinimidyl sulfoxide (DSSO),[16] protein interaction reporter (PIR),[17] and others represent a valid solution. By dissociating in the gas phase, they reveal the individual masses of the cross-linked peptides, reducing the software search space, and improve the sequencing of both peptides.[18−20] In this work, we remodeled the urea group of urea-based cross-linkers to an imide (Figure 1). This preserves the MS cleavability of imide-based reagents
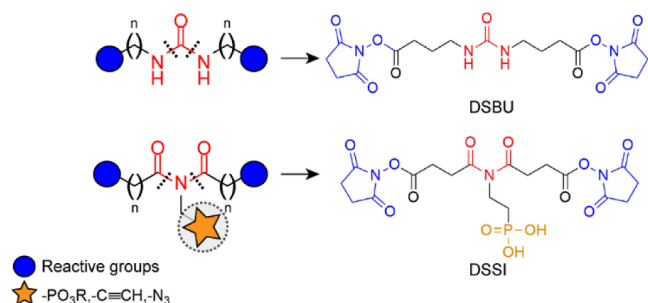

Figure 1. MS-cleavable urea DSBU and imide DSSI cross-linkers.

while the central nitrogen atom can be functionalized with affinity tags for cross-link enrichment. We introduce DSSI, a novel trifunctional MS-cleavable reagent containing a phosphonate handle for future IMAC enrichment of cross-links. We describe DSSI synthesis and studied in detail its behavior in the gas phase. We probed DSSI's reactivity in solution by cross-linking the intrinsically disordered protein (IDP) α-synuclein and a HEK293T cell lysate. We compared DSSI with DSBU at the same cross-link enrichment depth finding complementary structural information and protein−protein interactions (PPIs). DSSI cross-links underwent structure-based validation and yielded structural information on IDPs.

■ RESULTS AND DISCUSSION

Design and Synthesis of the DSSI Chemical Cross-Linker

Classical urea-based cross-linkers, such as DSBU, are unsuitable for accommodating an affinity tag without disrupting the molecule's symmetry. To overcome this limitation, we remodeled the central urea group into an imide. This enables the design of cross-linkers featuring a central trivalent nitrogen atom, ideal for attaching affinity handles. At the same time, imide-based cross-linkers preserve the MS cleavability and the spacer length modularity of their urea-based ancestors. DSSI, the first imide-based cross-linker, possesses the same C4 arms of DSBU and a central ethylene phosphonic acid group as an affinity tag. DSSI was synthesized using 2-amino ethanol **1** as the starting material (Figure 2). **1** was Boc-protected yielding **2** and used to prepare the cyclic ethylene sulfamidate **3**. Dibenzylphosphite sodium salt **4** was subsequently reacted with **3** to obtain the *tert*-butyl {2-[bis(benzyloxy)phosphoryl]ethyl}carbamate **5**. An acid-catalyzed deprotection resulted in the trifluoroacetyl (TFA) salt **6**. The latter was acylated and coupled to an imidazolide-activated *tert*-butyl succinic acid yielding the amide **7**. After this step, the *N*-hydroxysuccinimide (NHS) ester of *tert*-butyl succinate was used to obtain the di-*tert*-butyl imide derivative **8**. TFA deprotection of the *tert*-butyl groups yielded the diacid **9** which was esterified with NHS in the presence of 1-ethyl-3-(3-dimethylaminopropyl)carbodiimide (EDC). The resulting dibenzylphosphonic ester **10** was hydrogenated yielding the phosphonic acid **11** (4% overall yield), referred to as DSSI here. Synthesis details are provided in Figures S1 and S2.

Characterization of the Dissociation Behavior of DSSI upon Collisional Activation

DSBU-cross-linked products are cleaved upon collisional activation during MS/MS experiments, resulting in the cleavage of the N−CO bonds of the urea group. The dissociation generates an amine and an isocyanate fragment per peptide visible in fragment ion spectra as two doublets with a characteristic mass difference of ∼26 u.[4,15] Gas-phase dissociation of linear imides has not been systematically
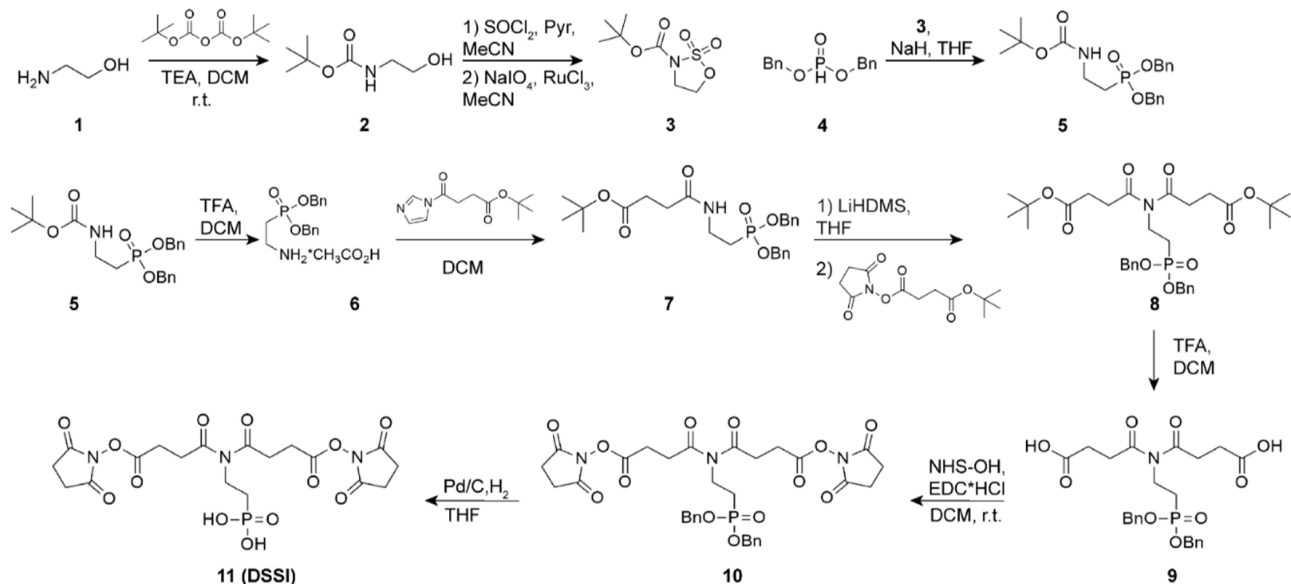

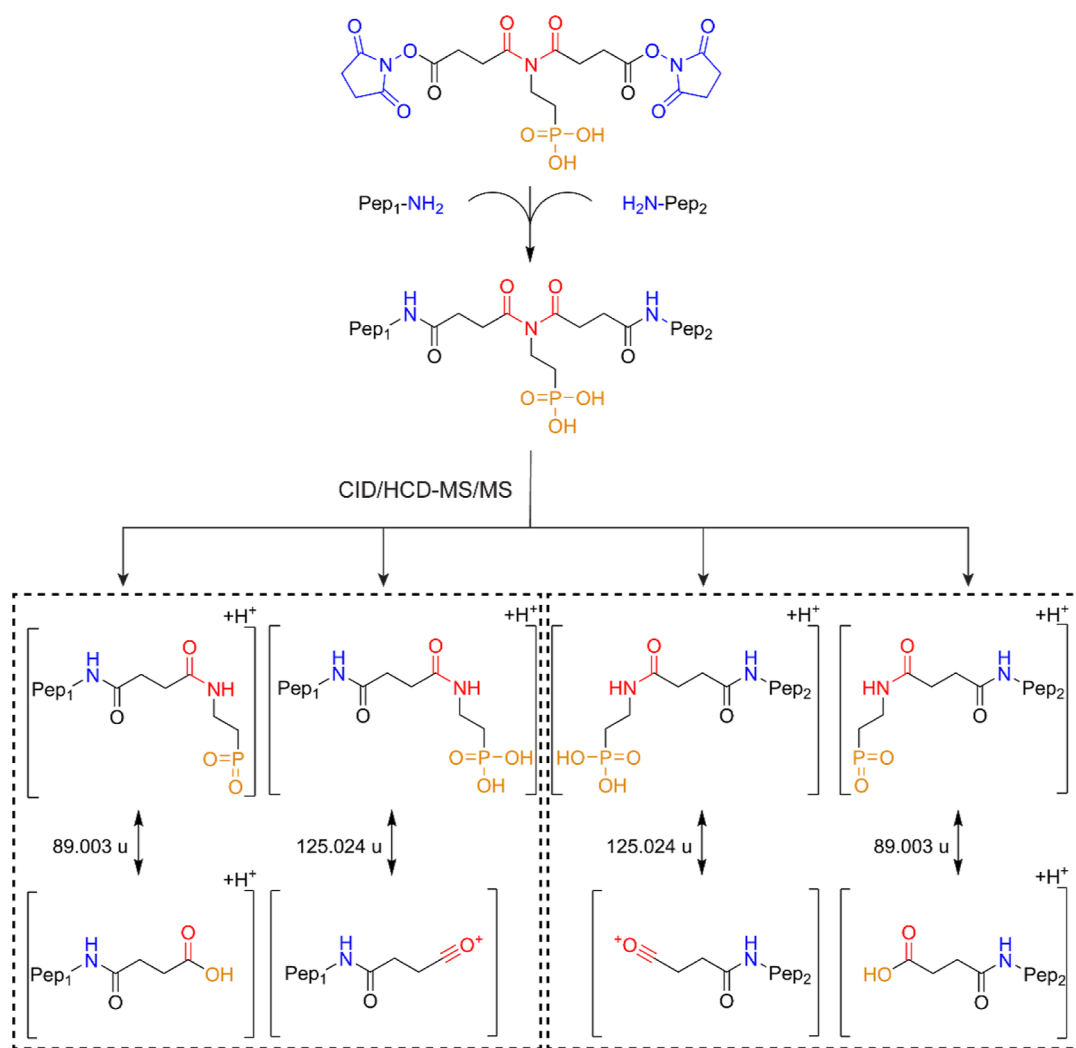**Figure 2.** Synthesis of the DSSI cross-linker.

Figure 3. Dissociation behavior of DSSI cross-links upon collisional activation. After the cross-linking reaction, two peptides in spatial proximity are covalently bridged by DSSI. Upon collisional activation, the central imide group dissociates, generating two sets of fragment ions for each cross-linked peptide. These doublets of signals in the fragment ion spectra have a mass difference of ~125 and ~89 u.

investigated previously. Nelson and McCloskey reported that, upon collisional activation, uracil and its derivatives[21] undergo ring opening via N−CO bond cleavage yielding an amide and a protonated acylium ion. We hypothesized DSSI to follow a similar fragmentation resulting in an MS-cleavable cross-linker. We applied DSSI to cross-link test peptide 1 (Ac-TRTESTDIKRASSREADYLINKER, Creative Molecules Inc.) and investigated its dissociation pattern upon collisional activation (Figure S3). Similar to cyclic imides, DSSI dissociates into ethylphosphonate amides and acylium ions (Figures 3 and S4A). Furthermore, one hydroxy group of the phosphonic acid rearranges intramolecularly yielding the dehydrated form of the ethylphosphonate amide fragment and a carboxylic acid fragment for each peptide (Figures 3 and S4B). Thus, DSSI cross-links generate two diagnostic doublets of signals in MS/MS experiments, spaced by ~89 and ~125 u (Figure 3). Neutral loss of water molecules from the precursor ion was observed at low collision energy (Figure S3A) and from the ethylphosphonate amide and the carboxylic acid fragments at higher collision energy (Figure S3B−D). MS/MS experiments of DSSI cross-links revealed that the optimal collision energy for linker and backbone fragmentation ranges between 25 and 35% normalized collision energy, similar to

that of DSBU (Figure S3). The comparable stabilities of the imide group of DSSI and of the amide bonds in the peptide backbone enable XL-MS analysis at the MS/MS level. This has been shown to increase scan rate and sensitivity compared to multistage MS (MS^n) methods.[22]

Additionally, DSSI generates characteristic reporter ions in the low m/z range, further enhancing confidence in cross-link identification (Figure S5).

Application of DSSI for Studying Single Proteins

The thorough characterization of DSSI gas-phase behavior enables the automated cross-link identification in complex samples by using the MeroX software.[23] We selected α-synuclein (α-syn) for assessing the reactivity of DSSI at physiological pH and to establish the downstream sample preparation workflow. α-syn is a small (14.5 kDa) IDP relevant in Parkinson's disease.[24] It consists of 140 amino acids and three domains, namely, the N-terminal lipid-binding domain, the central nonamyloid component domain, and C-terminal acidic domain. Upon α-syn cross-linking with DSSI, we applied in-solution proteolysis for 2 h with two consecutive additions of trypsin [fast in-solution digestion (ISD)],[25] and the resulting peptide mixture was analyzed by nano-LC-MS/MS
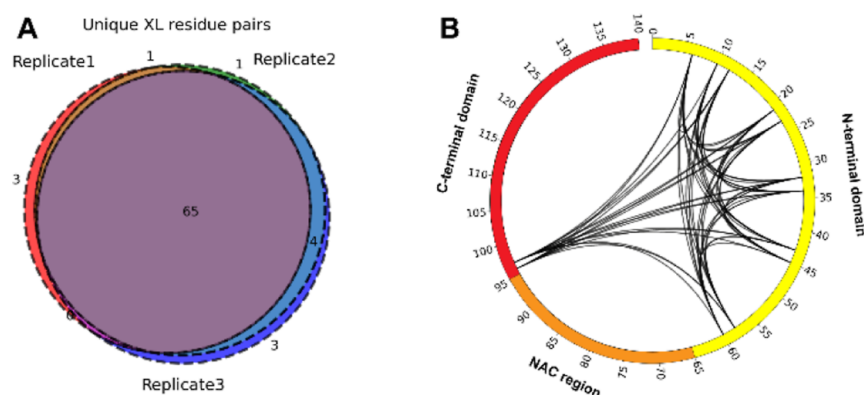
Figure 4. Application of DSSI for studying the intrinsically disordered α-synuclein. (A) Reproducibility of cross-linked residue pairs (Venn diagram). (B) Circos plot showing identified DSSI cross-links for α-synuclein.

(see Supporting Information for the experimental details). A MeroX search identified 77 unique residue pairs with ∼84% overlap across three replicates (Figure 4A). These were located within the N-terminal domain as well as between the N- and C-terminal regions of *α-syn* as has been observed with DSBU in our previous study (Figure 4B).[26] This suggests a comparable reactivity of the two cross-linkers. The high number of DSSI cross-links was achieved despite the application of fast ISD, while DSBU samples underwent overnight digestion (overnight ISD). We adopted the fast ISD for further DSSI cross-linking experiments.

Application of DSSI Cross-Linking to Cell Lysates

Before applying our protocol to more complex samples, we further evaluated fast ISD for HEK293T cell lysates and compared it to a standard overnight ISD. Both differently proteolyzed samples were separated by RP nano-HPLC and analyzed on a timsTOF Pro mass spectrometer (Figure S6). The fast ISD workflow enabled the identification of 5363 protein groups with 81% reproducibility over three replicates. This corresponds to only 6% fewer protein groups than those identified upon overnight ISD (5696 protein groups, corresponding to ∼80% reproducibility across three replicates) (Figure S6). The number of identified peptides was comparable between the two workflows (Figure S6B,C). Therefore, we decided to apply fast ISD to DSSI cross-linked samples to maximize the analysis throughput. We anticipate that reducing the time required for proteolysis will especially benefit the analysis throughput when including the affinity purification of imide-based cross-links. The latter will be addressed in a separate work. Here, our aim was to provide a comprehensive description of DSSI chemistry, comparing it with the well-characterized DSBU. For this reason, DSSI and DSBU cross-links were compared at the same enrichment depth, avoiding the IMAC/TiO$_2$ purification step of DSSI cross-links. Cross-linking of HEK293T cell lysates was performed at a total protein concentration of ∼1 g/L and 2 mM DSSI (see the Methods section for the experimental details). The resulting cross-links were compared to those observed when using DSBU and overnight ISD. Proteolyzed samples were fractionated by SEC to enrich cross-linked peptides (Figure S7A). Selected SEC fractions of each replicate were collected and individually subjected to LC-MS/MS analysis. MeroX analysis allowed the identification of 2478 unique DSSI cross-links related to 1241 proteins at a 1% false discovery rate for cross-link spectrum matches. Cross-links

were nonuniformly distributed over the SEC fractions analyzed, ranging from 147 to 1440 cross-links identified (Figure S7B). DSSI cross-links provide structural information on 582 PPIs in HEK293T cells. We compared DSSI cross-linked proteins to those targeted by DSBU for the HEK293T cell line. For this, proteins cross-linked by DSSI and DSBU were analyzed by the clusterProfiler R package[27] and classified based on gene ontology.[28−30] DSSI- and DBSU-cross-linked proteins were associated with the same cellular compartments of HEK293T cells, consistent with similar properties of the two cross-linkers (Figure S8A,B). In the case of molecular functions, proteins involved in chromatin, tubulin, and messenger RNA (mRNA)/ribosomal RNA (rRNA) binding were preferentially cross-linked by DSSI, while structural constituents of the cytoskeleton, proteins involved in ribonucleoprotein complex binding, NAD binding, and RNA helicases were preferentially cross-linked by DSBU (Figure S8C,D). By combining DSSI with DSBU, the cross-linked proteome and the cross-linking sites increase by 18 and 19%, respectively, compared to DSBU alone (Figure S9), enhancing the depth of structural data and the coverage of the PPI network in cells. Upon SEC enrichment, DSBU provided a higher number of unique cross-links.

Structure-Based Validation

DSSI has a similar spacer length as DSBU and is expected to covalently bridge residues with a maximum Cα−Cα distance of 35 Å.[31] We performed a structural validation of DSSI cross-links by mapping them into existing 3D models of three large protein complexes, namely, the chaperonin-containing TCP-1 (CCT) complex, the 26S proteasome, and the 80S ribosome (Figure 5A). The median distances observed ranged between 12 and 15 Å for both cross-linkers. 99% of DSSI cross-links were compatible with known high-resolution structures of the three protein assemblies (Figure 5B).

System-Wide Cross-Linking of IDPs

To further evaluate the structural information recapitulated by our cross-linking data, we focused on IDPs. Up to half of all human proteins contain structurally disordered regions, which present challenges for visualization using high-resolution methods.[32] The characterization of their highly dynamic structural ensembles requires integrative approaches, including XL-MS experiments. The key role of XL-MS in capturing the plasticity of IDPs is testified by our experiments on HEK293T cell lysates, where we identified intra- and interprotein cross-links involving 295 proteins listed in the DisProt database[33]
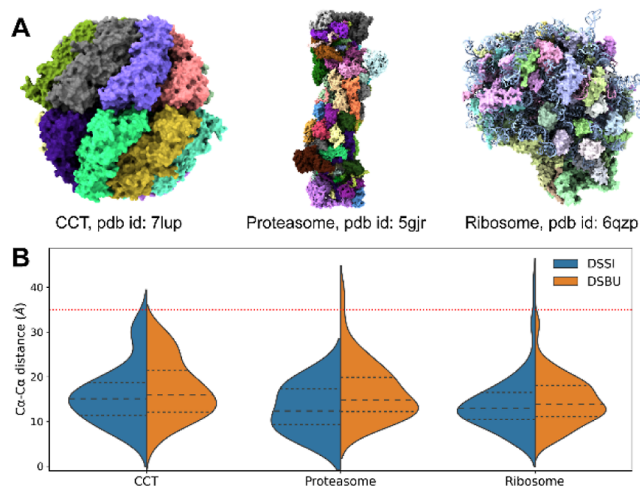
Figure 5. Structural XL-MS validation of DSSI cross-links. (A) Selected protein complexes: CCT, ~950 kDa; 26S proteasome, ~2.5 MDa; and 80S ribosome, ~4.5 MDa. (B) Violin plots comparing the $C\alpha-C\alpha$ distance distributions of DSSI (blue) and DSBU (orange) cross-links. Dashed and dotted lines represent the median and the interquartile ranges, respectively.

(Table S1). Specifically, 102 of them exhibit disordered content ranging from 20 to 100% (Table S2) including (i) transcription factors/repressors and their modulators (NF-κB, YY1, TP53BP1, and CREBBP), (ii) histones and their associated proteins (H4C1, H3-3A, H2BC11, HDAC1, and EP300), (iii) proteins involved in RNA binding/processing and splicing factors (SNRPA-B, SRRM1-2, SRSF1, and U2AF1), and (iv) ribosomal proteins/factors (SERBP1, RPLP2, RPL4, RPL24, ElF4B, and ElF4EBP1). Among those, we delved into the interactome of serpine1 mRNA-binding protein 1 (SERBP1, also known as plasminogen activator inhibitor 1 RNA-binding protein). SERBP1 is a ~45 kDa RNA-binding protein involved in mRNA maturation, translational regulation, and various biological functions.[34,35] SERBP1−ribosome binding promotes ribosome hibernation.[36] SERBP1 is an IDP (see Figure 6A, according to IUPRED and DISPRED disorder predictions[37,38]) with a short α-helix comprising residues 290−300. This α-helix has been confirmed by NMR[34] and predicted by AlphaFold2[39] with high confidence (Figure 6B). As the conformational flexibility of IDPs does not hamper their chemical reactivity, we were able to identify 10 unique SERBP1 cross-links, recapitulating the interaction of all its structural regions with 7 binding proteins (Figure 6C). Initially, we mapped the cross-link between Lys 299 of SERBP1 and Lys 116 of the 40S Ribosomal Protein S12 (RPS12). With a $C\alpha-C\alpha$ distance of 10 Å, this cross-link aligns well with the cryo-EM structure of the 80S ribosome,[40] confirming the localization of SERBP1's sole visualized α-helix in this protein complex (pdb id 6z6m, Figure 6D). Furthermore, we found (i) the N-terminal region of SERBP1 interacting with RPS3A, RPS9, RPS14, and RPS28 and (ii) the C-terminal domain interacting with RPS15 and RACK1, a scaffold protein involved in SERBP1 recruitment.[41] These PPIs possess a high STRING score and some of them have been identified in previous studies.[36,42] We observed that SERBP1
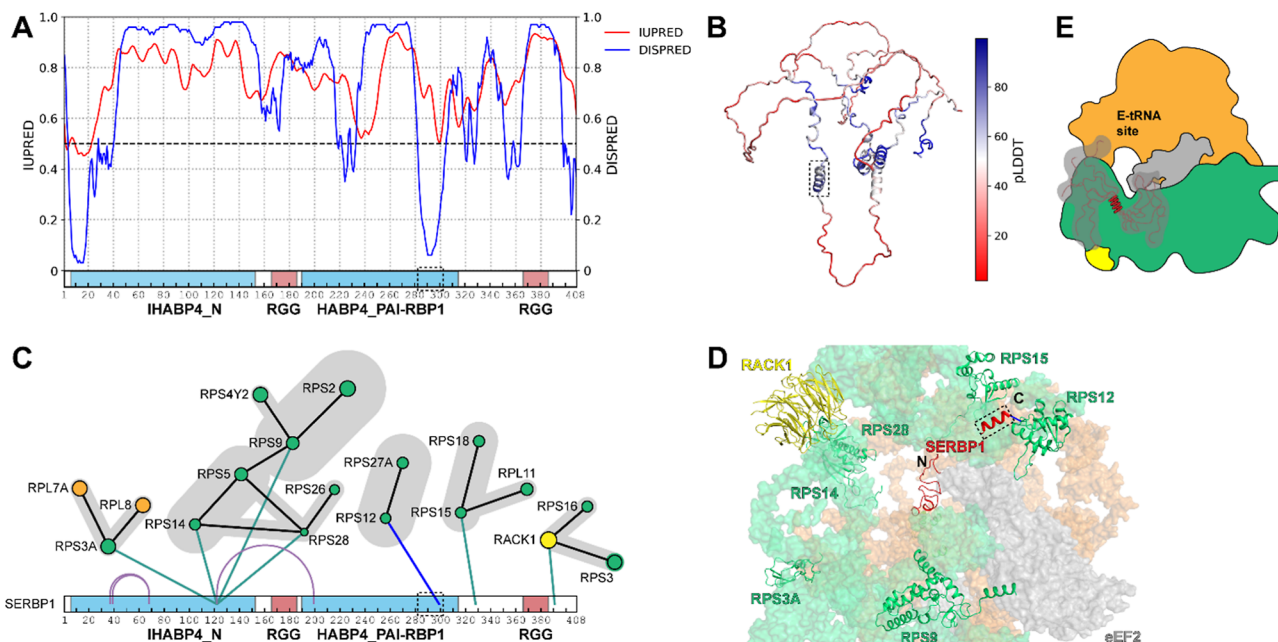

Figure 6. Evaluation of PPIs involving the IDP SERBP1. (A) IUPRED and DISOPRED disorder predictions of SERBP1, confirming its high disordered nature. The horizontal bar displays the SERBP1 sequence number and domain annotation. (B) AlphaFold2 model of SERBP1, with the experimentally confirmed α-helix (dashed rectangle) spanning residues 290−300. (C) SERBP1 interprotein cross-links to several ribosomal proteins of the 40S subunit. The cross-link involving SERBP1 solved helix (dashed rectangle) with RPS12 is colored in blue. (D) Bottom view of the cryo-EM structure of the 80S ribosome (pdb id 6z6m), showing the only mappable cross-link between SERBP1 helix and RPS12. All other cross-links involved unsolved regions in either SERBP1 or ribosomal proteins. Proteins of the 40S subunit are depicted in green, proteins of the 60S subunit in orange, RACK1 in yellow, and eEF2 and other associated factors in gray. RNA is not shown for clarity. (E) Schematic cartoon representation of the dynamic nature of the interaction between SERBP1 and ribosome. The high disorder content allows SERBP1 to sample a vast ensemble of conformations; SERBP1 binds to the mRNA entry channel and the A and P sites of the small 40S subunit (where it interacts with eEF2, in gray), inhibiting translation.

can occupy a broad surface of the 40S ribosomal subunit, sampling a large conformational ensemble at the mRNA entry channel, as well as the A and P sites of the ribosome, thereby inhibiting translation (Figure 6E). This plasticity was also observed for SERBP1 homologues[40,43,44] suggesting that intrinsic disorder plays a pivotal role for the regulatory functions of these hibernation factors.

■ CONCLUSIONS

We synthesized and applied DSSI as the first imide-based cross-linker for protein 3D-structural analysis and proteome-wide interaction studies. This novel class of cross-linkers harbors an affinity tag for affinity purification of cross-links. In particular, DSSI maintains the NHS ester warheads and the spacer length of the widely used DSBU but possesses a phosphonate handle for IMAC or TiO_2 cross-link enrichment. We deciphered the gas-phase chemistry of DSSI and parameterized its MS cleavability for automated cross-link identification. Its diagnostic fragment ion doublets can be recognized by the MeroX software for a fast and reliable identification of cross-links in highly complex samples. Furthermore, we demonstrated the reactivity of DSSI by cross-linking α-syn and HEK293T cell lysates. In total, we identified 2478 unique cross-links involving 1241 proteins. DSSI targets proteins in a wide range of cellular compartments and expands the scope of XL-MS. DSSI cross-links were validated based on the high-resolution structures of three large protein complexes, the CCT complex, the 26S proteasome, and the 80S ribosome. The $C\alpha-C\alpha$ distance distribution of DSSI cross-links matches that of DSBU. Beyond characterizing PPIs in HEK293T cells, we derived morphological insights into IDPs, such as SERBP1. We anticipate that the MS-cleavable DSSI and other imide-based cross-linkers, in combination with SEC and IMAC enrichment of cross-link products, will contribute to unveiling structural details of the cell interactome. Future studies will be directed to address the IMAC enrichment.

■ METHODS

Test Peptide 1 Cross-Linking with DSSI

A solution containing 50 μM test peptide 1 in 50 mM HEPES, pH 8.5 was incubated at room temperature for 1 h with 1 mM DSSI. The cross-linker was dissolved in neat dimethyl sulfoxide (DMSO) immediately before adding it to the peptide solution. The reaction was quenched by adding ammonium bicarbonate (ABC) to a final concentration of 20 mM.

α-Synuclein Cross-Linking with DSSI

α-Synuclein was expressed and purified as stated previously.[1] In brief, recombinant production of N-terminally acetylated α-synuclein (α-syn) was performed by coexpression of α-syn with N-terminal acetylase B (NatB). The α-syn gene was ligated into a pET21a(+) vector using the XhoI and NdeI restriction sites. The pTSAra-NatB plasmid was kindly provided by Tim Bartels (Harvard Medical School) for coexpression. *Escherichia coli* BL21(DE3) cells were transformed with both plasmids. Cell growth and expression steps were carried out as described previously.[45] α-Syn was purified with a two-step protocol consisting of a first anion-exchange chromatography step, followed by SEC. Fractions containing α-syn were flash-frozen in liquid nitrogen and thawed on ice before doing the cross-linking experiments. A solution containing 10 μM α-synuclein in 50 mM HEPES, pH 7.4 was incubated at room temperature for 1 h with 1 mM DSSI. The cross-linker was dissolved in neat DMSO immediately before adding it to the protein solution. The reaction was quenched by adding ABC to a final concentration of 20 mM.

HEK293T Cross-Linking with DSSI/DSBU

HEK293T cells were cultured in Dulbecco's modified Eagle's medium supplemented with 10% fetal bovine serum. After washing with phosphate buffered saline three times, cell pellets were resuspended in the cross-linking buffer (20 mM HEPES, 10 mM MgCl2, 150 mM KCl, 1%v/v DDM, pH 7.4). Cell debris was removed by centrifugation at 13,000*g* for 15 min at 4 °C. The supernatant was collected and adjusted to a final concentration of 1 mg/mL before carrying out the cross-linking reaction. 2 mM DSSI or DSBU was added and the reaction mixture was incubated for 1h at room temperature. The cross-linker was dissolved in neat DMSO immediately before adding it to the cell lysate. The reaction was quenched by adding ABC to a final concentration of 20 mM.

■ ASSOCIATED CONTENT

ⓈⒾ Supporting Information

The Supporting Information is available free of charge at https://pubs.acs.org/doi/10.1021/jacsau.4c00282.

> Experimental details including synthesis and characterization of DSSI, cross-linking, enzymatic digestion, SEC, and data analysis (PDF)
> Tables of cross-linked IDPs (XLSX)
> MS data deposited to the ProteomeXchange Consortium via the PRIDE partner repository with the project accession PXD050960 (XLSX)

■ AUTHOR INFORMATION

Corresponding Author

Claudio Iacobucci − *Center for Structural Mass Spectrometry, Martin Luther University Halle-Wittenberg, Halle/Saale D-01620, Germany; Department of Pharmaceutical Chemistry and Bioanalytics, Institute of Pharmacy, Martin Luther University Halle-Wittenberg, Halle/Saale D-01620, Germany; Department of Physical and Chemical Sciences, University of L'Aquila, Coppito II 67100 L'Aquila, Italy;* ⓞ orcid.org/0000-0001-9592-3606; Email: claudio.iacobucci@univaq.it

Authors

Alessio Di Ianni − *Department of Pharmaceutical Chemistry and Bioanalytics, Institute of Pharmacy, Martin Luther University Halle-Wittenberg, Halle/Saale D-01620, Germany; Center for Structural Mass Spectrometry, Martin Luther University Halle-Wittenberg, Halle/Saale D-01620, Germany*

Christian H. Ihling − *Department of Pharmaceutical Chemistry and Bioanalytics, Institute of Pharmacy, Martin Luther University Halle-Wittenberg, Halle/Saale D-01620, Germany; Center for Structural Mass Spectrometry, Martin Luther University Halle-Wittenberg, Halle/Saale D-01620, Germany*

Tomáš Vranka − *CF Plus Chemicals s.r.o., Brno-Řečkovice 621 00, Czechia*

Václav Matoušek − *CF Plus Chemicals s.r.o., Brno-Řečkovice 621 00, Czechia*

Andrea Sinz − *Department of Pharmaceutical Chemistry and Bioanalytics, Institute of Pharmacy, Martin Luther University Halle-Wittenberg, Halle/Saale D-01620, Germany; Center for Structural Mass Spectrometry, Martin Luther University Halle-Wittenberg, Halle/Saale D-01620, Germany;* ⓞ orcid.org/0000-0003-1521-4899

Complete contact information is available at:

Author Contributions

The manuscript was written through contributions of all authors. All authors have given approval to the final version of the manuscript. CRediT: **Christian H. Ihling** formal analysis, methodology, writing-original draft; **Václav Matoušek** conceptualization, methodology; **Andrea Sinz** conceptualization, funding acquisition, supervision, writing-original draft; **Claudio Iacobucci** conceptualization, funding acquisition, supervision, writing-original draft.

Notes

The authors declare no competing financial interest.

REFERENCES

(1) Piersimoni, L.; Kastritis, P. L.; Arlt, C.; Sinz, A. Cross-Linking Mass Spectrometry for Investigating Protein Conformations and Protein-Protein Interactions—A Method for All Seasons. *Chem. Rev.* **2022**, *122* (8), 7500−7531.

(2) Sinz, A. Cross-Linking/Mass Spectrometry for Studying Protein Structures and Protein-Protein Interactions: Where Are We Now and Where Should We Go from Here? *Angew Chem. Int. Ed. Engl.* **2018**, *57* (22), 6390−6396.

(3) O'Reilly, F. J.; Graziadei, A.; Forbrig, C.; Bremenkamp, R.; Charles, K.; Lenz, S.; Elfmann, C.; Fischer, L.; Stülke, J.; Rappsilber, J. Protein complexes in cells by AI-assisted structural proteomics. *Mol. Syst. Biol.* **2023**, *19* (4), No. e11544.

(4) Götze, M.; Iacobucci, C.; Ihling, C. H.; Sinz, A. A Simple Cross-Linking/Mass Spectrometry Workflow for Studying System-wide Protein Interactions. *Anal. Chem.* **2019**, *91* (15), 10236−10244.

(5) Lenz, S.; Sinn, L. R.; O'Reilly, F. J.; Fischer, L.; Wegner, W.; Rappsilber, J. Reliable identification of protein-protein interactions by crosslinking mass spectrometry. *Nat. Commun.* **2021**, *12* (1), 3564.

(6) Giese, S. H.; Sinn, L. R.; Wegner, F.; Rappsilber, J. Retention time prediction using neural networks increases identifications in crosslinking mass spectrometry. *Nat. Commun.* **2021**, *12*, 3237.

(7) Jiao, F.; Yu, C.; Wheat, A.; Wang, X.; Rychnovsky, S. D.; Huang, L. Two-Dimensional Fractionation Method for Proteome-Wide Cross-Linking Mass Spectrometry Analysis. *Anal. Chem.* **2022**, *94* (10), 4236−4242.

(8) Iacobucci, C.; Götze, M.; Ihling, C. H.; Piotrowski, C.; Arlt, C.; Schäfer, M.; Hage, C.; Schmidt, R.; Sinz, A. A cross-linking/mass spectrometry workflow based on MS-cleavable cross-linkers and the MeroX software for studying protein structures and protein-protein interactions. *Nat. Protoc.* **2018**, *13* (12), 2864−2889.

(9) Burke, A. M.; Kandur, W.; Novitsky, E. J.; Kaake, R. M.; Yu, C.; Kao, A.; Vellucci, D.; Huang, L.; Rychnovsky, S. D. Synthesis of two new enrichable and MS-cleavable cross-linkers to define protein-protein interactions by mass spectrometry. *Org. Biomol. Chem.* **2015**, *13* (17), 5030−5037.

(10) Stadlmeier, M.; Runtsch, L. S.; Streshnev, S.; Wühr, M.; Carell, T. A Click-Chemistry-Based Enrichable Crosslinker for Structural and Protein Interaction Analysis by Mass Spectrometry. *Chembiochem.* **2020**, *21* (1-2), 103−107.

(11) Steigenberger, B.; Pieters, R. J.; Heck, A. J. R.; Scheltema, R. A. PhoX: An IMAC-Enrichable Cross-Linking Reagent. *ACS Cent. Sci.* **2019**, *5* (9), 1514−1522.

(12) Jiang, P.-L.; Wang, C.; Diehl, A.; Viner, R.; Etienne, C.; Nandhikonda, P.; Foster, L.; Bomgarden, R. D.; Liu, F. A Membrane-Permeable and Immobilized Metal Affinity Chromatography (IMAC) Enrichable Cross-Linking Reagent to Advance In Vivo Cross-Linking Mass Spectrometry. *Angew. Chem., Int. Ed. Engl.* **2022**, *61*, No. e2021139.

(13) Gao, H.; Zhao, L.; Zhong, B.; Zhang, B.; Gong, Z.; Zhao, B.; Liu, Y.; Zhao, Q.; Zhang, L.; Zhang, Y. In-Depth In Vivo Crosslinking in Minutes by a Compact, Membrane-Permeable, and Alkynyl-Enrichable Crosslinker. *Anal. Chem.* **2022**, *94* (21), 7551−7558.

(14) Gao, H.; Zhao, Q.; Gong, Z.; Zhong, B.; Chen, J.; Sui, Z.; Li, X.; Liang, Z.; Zhang, Y.; Zhang, L. Alkynyl-Enrichable Carboxyl-Selective Crosslinkers to Increase the Crosslinking Coverage for Deciphering Protein Structures. *Anal. Chem.* **2022**, *94* (36), 12398−12406.

(15) Müller, M. Q.; Dreiocker, F.; Ihling, C. H.; Schäfer, M.; Sinz, A. Cleavable cross-linker for protein structure analysis: reliable identification of cross-linking products by tandem MS. *Anal. Chem.* **2010**, *82* (16), 6958−6968.

(16) Kao, A.; Chiu, C.; Vellucci, D.; Yang, Y.; Patel, V. R.; Guan, S.; Randall, A.; Baldi, P.; Rychnovsky, S. D.; Huang, L. Development of a novel cross-linking strategy for fast and accurate identification of cross-linked peptides of protein complexes. *Mol. Cell. Proteomics* **2011**, *10* (1), M110.002170.

(17) Tang, X.; Munske, G. R.; Siems, W. F.; Bruce, J. E. Mass Spectrometry Identifiable Cross-Linking Strategy for Studying Protein-Protein Interactions. *Anal. Chem.* **2005**, *77*, 311−318.

(18) Piersimoni, L.; Sinz, A. Cross-linking/mass spectrometry at the crossroads. *Anal. Bioanal. Chem.* **2020**, *412* (24), 5981−5987.

(19) Kolbowski, L.; Lenz, S.; Fischer, L.; Sinn, L. R.; O'Reilly, F. J.; Rappsilber, J. Improved Peptide Backbone Fragmentation Is the Primary Advantage of MS-Cleavable Crosslinkers. *Anal. Chem.* **2022**, *94* (22), 7779−7786.

(20) Sinz, A. Divide and conquer: cleavable cross-linkers to study protein conformation and protein-protein interactions. *Anal. Bioanal. Chem.* **2017**, *409* (1), 33−44.

(21) Nelson, C. C.; McCloskey, J. A. Collision-induced dissociation of uracil and its derivatives. *J. Am. Soc. Mass. Spectrom.* **1994**, *5* (5), 339−349.

(22) Stieger, C. E.; Doppler, P.; Mechtler, K. Optimized Fragmentation Improves the Identification of Peptides Cross-Linked by MS-Cleavable Reagents. *J. Proteome Res.* **2019**, *18* (3), 1363−1370.

(23) Götze, M.; Pettelkau, J.; Fritzsche, R.; Ihling, C. H.; Schäfer, M.; Sinz, A. Automated assignment of MS/MS cleavable cross-links in protein 3D-structure analysis. *J. Am. Soc. Mass Spectrom.* **2015**, *26* (1), 83−97.

(24) Stefanis, L. α-Synuclein in Parkinson's Disease. *Cold Spring Harb. Perspect. Med.* **2012**, *2* (2), a009399.

(25) Matzinger, M.; Müller, E.; Dürnberger, G.; Pichler, P.; Mechtler, K. Robust and Easy-to-Use One-Pot Workflow for Label-Free Single-Cell Proteomics. *Anal. Chem.* **2023**, *95* (9), 4435−4445.

(26) Ubbiali, D.; Fratini, M.; Piersimoni, L.; Ihling, C. H.; Kipping, M.; Heilmann, I.; Iacobucci, C.; Sinz, A. Direct Observation of ″Elongated″ Conformational States in α-Synuclein upon Liquid-Liquid Phase Separation. *Angew. Chem., Int. Ed. Engl.* **2022**, *61* (46), No. e202205726.

(27) Yu, G.; Wang, L.-G.; Han, Y.; He, Q.-Y. clusterProfiler: an R Package for Comparing Biological Themes Among Gene Clusters. *OMICS* **2012**, *16* (5), 284−287.

(28) The Gene Ontology Consortium Michael, A.; Ball, C. A.; Blake, J. A.; Botstein, D.; Butler, H.; Michael Cherry, J.; Davis, A. P.; Dolinski, K.; Dwight, S. S.; Eppig, J. T.; Harris, M. A.; Hill, D. P.; Issel-Tarver, L.; Kasarskis, A.; Lewis, S.; Matese, J. C.; Richardson, J. E.; Ringwald, M.; Rubin, G. M.; Sherlock, G. Gene Ontology: tool for the unification of biology. *Nat. Genet.* **2000**, *25* (1), 25−29.

(29) Jiao, F.; Salituro, L. J.; Yu, C.; Gutierrez, C. B.; Rychnovsky, S. D.; Huang, L. Exploring an Alternative Cysteine-Reactive Chemistry to Enable Proteome-Wide PPI Analysis by Cross-Linking Mass Spectrometry. *Anal. Chem.* **2023**, *95* (4), 2532−2539.

(30) Jiao, F.; Yu, C.; Wheat, A.; Chen, L.; Mamie Lih, T.-S.; Zhang, H.; Huang, L. DSBSO-Based XL-MS Analysis of Breast Cancer PDX Tissues to Delineate Protein Interaction Network in Clinical Samples. *J. Proteome Res.* **2024**, DOI: 10.1021/acs.jproteome.3c00832.

(31) Di Ianni, A.; Tüting, C.; Kipping, M.; Ihling, C. H.; Köppen, J.; Iacobucci, C.; Arlt, C.; Kastritis, P. L.; Sinz, A. Structural assessment of the full-length wild-type tumor suppressor protein p53 by mass spectrometry-guided computational modeling. *Sci. Rep.* **2023**, *13* (1), 8497.

(32) Xue, B.; Dunker, A. K.; Uversky, V. N. Orderly order in protein intrinsic disorder distribution: disorder in 3500 proteomes from viruses and the three domains of life. *J. Biomol. Struct. Dyn.* **2012**, *30* (2), 137−149.

(33) Sickmeier, M.; Hamilton, J. A.; LeGall, T.; Vacic, V.; Cortese, M. S.; Tantos, A.; Szabo, B.; Tompa, P.; Chen, J.; Uversky, V. N.; Obradovic, Z.; Dunker, A. K. DisProt: the Database of Disordered Proteins. *Nucleic Acids Res.* **2007**, *35*, D786−D793.

(34) Baudin, A.; Moreno-Romero, K.; Xu, X.; Selig, E.; Penalva, O. F.; Libich, D. S. Structural Characterization of the RNA-Binding Protein SERBP1 Reveals Intrinsic Disorder and Atypical RNA Binding Modes. *Front. Mol. Biosci.* **2021**, *8*, 744707.

(35) Muto, A.; Sugihara, Y.; Shibakawa, M.; Oshima, K.; Matsuda, T.; Daita, N. The mRNA-binding protein Serbp1 as an auxiliary protein associated with mammalian cytoplasmic ribosomes. *Cell Biochem Funct.* **2018**, *36*, 312−322.

(36) Kipper, K.; Mansour, A.; Pulk, A. Neuronal RNA granules are ribosome complexes stalled at the pre-translocation state. *J. Mol. Biol.* **2022**, *434* (20), 167801.

(37) Dosztányi, Z. Prediction of protein disorder based on IUPred. *Protein Sci.* **2018**, *27* (1), 331−340.

(38) Ward, J. J.; McGuffin, L. J.; Bryson, K.; Buxton, B. F.; Jones, D. T. The DISOPRED server for the prediction of protein disorder. *Bioinformatics* **2004**, *20* (13), 2138−2139.

(39) Jumper, J.; Evans, R.; Pritzel, A.; Green, T.; Figurnov, M.; Ronneberger, O.; Tunyasuvunakool, K.; Bates, R.; Žídek, A.; Potapenko, A.; Bridgland, A.; Meyer, C.; Kohl, S. A. A.; Ballard, A. J.; Cowie, A.; Romera-Paredes, B.; Nikolov, S.; Jain, R.; Adler, J.; Back, T.; Petersen, S.; Reiman, D.; Clancy, E.; Zielinski, M.; Steinegger, M.; Pacholska, M.; Berghammer, T.; Bodenstein, S.; Silver, D.; Vinyals, O.; Senior, A. W.; Kavukcuoglu, K.; Kohli, P.; Hassabis, D. Highly accurate protein structure prediction with AlphaFold. *Nature* **2021**, *596* (7873), 583−589.

(40) Wells, J. N.; Buschauer, R.; Mackens-Kiani, T.; Best, K.; Kratzat, H.; Berninghausen, O.; Becker, T.; Gilbert, W.; Cheng, J.; Beckmann, R. Structure and function of yeast Lso2 and human CCDC124 bound to hibernating ribosomes. *PLoS Biol.* **2020**, *18* (7), No. e3000780.

(41) Bolger, G. B. The RNA-binding protein SERBP1 interacts selectively with the signaling protein RACK1. *Cell Signal.* **2017**, *35*, 256−263.

(42) Liu, F.; Rijkers, D. T. S.; Post, H.; Heck, A. J. R. Proteome-wide profiling of protein assemblies by cross-linking mass spectrometry. *Nat. Methods* **2015**, *12* (12), 1179−1184.

(43) Anger, A. M.; Armache, J.-P.; Berninghausen, O.; Habeck, M.; Subklewe, M.; Wilson, D. N.; Beckmann, R. Structures of the human and Drosophila 80S ribosome. *Nature* **2013**, *497* (7447), 80−85.

(44) Brown, A.; Baird, M. R.; Yip, M. C.; Murray, J.; Shao, S. Structures of translationally inactive mammalian ribosomes. *Elife* **2018**, *7*, No. e40486.

(45) Powers, A. E.; Patel, D. S. Expression and Purification of Untagged α-Synuclein. *Methods Mol. Biol.* **2019**, *1948*, 261−269.